A Low-Complexity Algorithm for NB-IoT Networks

Salem Alemaishat
School of Computing and Informatics, Al-Hussein Technical University KHBP, Amman 11855, Jordan

Keywords: NB-IoT, 5G, 3GPP, Algorithms.

Abstract: The NB-IoT is a brand-new narrowband IoT technology based on cellular networks. It is an international standard defined by the 3GPP organization. It can be widely deployed worldwide. It focuses on low-power wide area networks and operates based on licensed spectrum. It can be directly deployed in The LTE network has low deployment costs and smooth upgrade capabilities. One of the most influencing factor in NB-IoT networks is time delay, which affects the system performance. Therefore, this paper proposes an efficient algorithm to estimate such factor based on the idea of ICI cancellation method to gradually mitigate the interference between signals in each cell. The proposed algorithm deploys time-frequency cross-correlation overlapping in each iteration based on the conventional correlation method to further enhance the time delay estimation accuracy. Furthermore, based on the noise threshold, a first arrival path algorithm is proposed to eradicate the multipath fading. Simulation results show that the proposed algorithm can effectively improve the time delay as compared with existing algorithms.

1 INTRODUCTION

The Narrowband Internet of Things (NB-IoT) proposed in the 3GPP R14 standard supports the following base station settings:

Position method: Global Assisted Positioning Satellite System (A-GNSS), E-CID (E-UTRAN cell identifier), downlink positioning method based on Observed Time Difference of Arrival (OTDOA) or uplink based on Observed Time Difference of Arrival (UTDOA) Positioning method Staniec (2020). Taking comprehensive consideration of terminal complexity, network capacity, cost and resources, and positioning scenarios, if the OTDOA positioning method is adaptively improved, it can make it more universal than other positioning methods and more suitable for a large number of NB-IoT nodes The positioning cost requirements. The positioning method based on OTDOA mainly measures the time delay estimation (TDE) value of 3 or more cell positioning reference signals (PRS) reaching the positioning terminal, and estimates the position of the terminal when the position of each base station is known. Delay estimation is a very important factor in the positioning of NB-IoT based on OTDOA.

The representative of the classic delay estimation algorithm is the cross-correlation method (Knapp, 2003), which estimates the signal delay by searching for the correlation peak between the local PRS signal and the received signal. Power consumption and low cost are required, but the accuracy of time delay estimation is seriously affected by the system sampling rate, which makes it not suitable for accurate positioning of NB-IoT devices with a low sampling rate (i.e. 1.92 MHz). The super-resolution delay estimation algorithm (Deng, 2020; Saraereh, 2020; Gu, 2017) increases the cost of IoT devices due to complexity issues and affects its power consumption. In addition, due to the building and terrain, the structure of the mobile communication channel is complicated. The PRS signals sent by different cells reach the positioning terminal through multiple paths. In this process, the signals between the cells interfere with each other, and the signals in the cells are also due to multipath effects. Will be affected by non-line-of-sight (NLOS) (Shahjehan, 2020), these factors will cause delay estimation errors and even obvious errors. Many scholars have proposed some algorithms to suppress the influence of NLOS and eliminate inter-cell interference (Lee, 2018; Khan, 2018; Hu, 2017), but most of these algorithms are more complex, such as the continuous interference elimination based on expectation maximization (EM-SIC) Algorithm, which will cause relatively large system overhead. Although some existing time delay estimation algorithms based on cross-correlation (Ye, 2016; Sun, 2016; Jameel, 2019) have improved accuracy, they fail to

Alemaishat, S.
A Low-Complexity Algorithm for NB-IoT Networks.
DOI: 10.5220/0010439802050214
In *Proceedings of the 6th International Conference on Internet of Things, Big Data and Security (IoTBDS 2021)*, pages 205-214
ISBN: 978-989-758-504-3

systematically consider inter-cell signal interference and NLOS effects.

In response to the above problems and combined with the 3GPP R14 standard, this paper proposes a delay estimation algorithm based on inter-cell interference cancellation. On the one hand, the algorithm separates the delay estimation of the serving base station and neighboring base stations, first reconstructs the received signal from the serving base station, and on this basis, eliminates the strong interference of the serving base station signal, and then uses the iterative continuous interference cancellation algorithm to gradually remove the received signal. The mutual interference between signals from neighboring base stations. On the other hand, in order to break through the limitation of low sampling rate, this algorithm proposes a time-frequency cross-correlation overlapping delay estimation algorithm (F&T_TDE) on the basis of traditional correlation algorithms, which mainly includes the following two stages:

In the first stage, multiple OFDM symbols are combined to obtain a preliminary time delay estimation value using related algorithms, and the first path search algorithm based on noise threshold is used to suppress the impact of multipath effects.

In the second stage, a part of the received signal is selected for interpolation processing to obtain an accurate time delay estimate. In addition, considering the extreme conditions in the project implementation, there may be less than 3 locating base stations, which makes the algorithm proposed in this paper unable to estimate the location of the terminal equipment. An auxiliary positioning algorithm to deal with such situations. Common non-base station positioning algorithms include GPS positioning, anchor node positioning, fingerprint positioning and other methods. Taking into account the low power consumption, low-cost characteristics of NB-IoT, and the total cost of positioning, the introduction of anchor node positioning is more practical. Finally, several commonly used performance indicators of the time delay estimation algorithm and the performance of auxiliary positioning are analyzed through simulation, and the feasibility of the proposed algorithm is verified.

2 SYSTEM MODEL

According to the 3GPP protocol (Staniec (2020)), the PRS signal should be transmitted in N_{PRS} consecutive positioning subframes, where N_{PRS} is configured by a higher-level protocol, referring to the principle of PRS generation in the 3GPP protocol, it can be obtained that when $lN \leq n < (l+1)N$, the time domain PRS signal is

$$s'_{p,l}(n) = \frac{1}{\sqrt{N}} \sum_{k=0}^{N-1} S_{p,l}(k) e^{j\frac{2\pi nk}{N}} \tag{1}$$

Among them, $p = 0$ indicates that the signal comes from the serving base station, $p = 1, 2, \ldots, P-1$ P indicates the number of base stations involved in positioning) indicates that the signal comes from different neighboring base stations. A wireless subframe has 2 time slots, and a time slot includes 7 OFDM symbols, then the number of OFDM symbols in a positioning subframe is $L = 14$, $l \in \{0,1,2,\ldots,L\}$. N represents the length of inverse fast Fourier transform (IFFT); $S_{p,l}(k)$ is the frequency domain PRS signal corresponding to the l OFDM symbol of the p base station after resource mapping. After adding a guard interval of N_{CP} in length, the corresponding PRS signal sent in the time domain is expressed as, $S_{p,l}(n)$. The transmitted signal reaches the receiving end through M paths, and the received signal in the time domain of path m for the lth OFDM symbol corresponding to the NB-IoT device terminal is

$$y_{p,m}^{l}(n) = \beta_p^m h_p^m(n) s_{p,l}(n - \tau_{p,m}) \tag{2}$$

Where, $lN' \leq n < (l+1)N'$, $N' = N + N_{CP}$; $h_p^m(n) = h_p^m e^{j\frac{2\pi n}{N'}}$, β_p^m and h_p^m are the amplitude attenuation factor and initial amplitude of the mth branch of the signal sent by the pth cell, respectively; $\tau_{p,m}$ is the delay number of the branch path. Adding the noise $w(n)$ in the channel, the final total signal received at the equipment terminal is

$$y(n) = \sum_{p=0}^{P-1} \sum_{m=0}^{M-1} \sum_{l=0}^{L-1} y_{p,m}^{l}(n) + w(n) \tag{3}$$

Let $r_{p,l}(n)$ denote the signal, $s_{p,l}(n)$ and the cross-correlation function of $y(n)$, as shown in equation (4).

$$r_{p,l}(n) = E\left[s_{p,l}(n) y(n)\right] = R_s\left(n - \tau_{p,l}\right) \tag{4}$$

From the Hermit property of the autocorrelation function and the characteristic that the origin reaches the maximum value (Jabeen (2019)), that is

$$\begin{cases} R_s(\tau) = R_s^*(-\tau) \\ |R_s(\tau)| \leq R_s(0) \end{cases} \tag{5}$$

It can be seen from equation (5) that when $n = \tau_{p,l}$, then $r_{p,l}(n)$ takes the maximum value, and the initial delay number $\tau_{p,\text{init}}$ is subtracted, and finally the delay estimate is obtained, $\hat{t}_{p,l}$ is shown in equation (6).

$$\hat{t}_{p,l} = \left(\tau_{p,l} - \tau_{p,\mathrm{init}}\right) T_{\mathrm{s}} \tag{6}$$

Among them, T_{s} represents the time interval of sampling points.

3 PROPOSED ALGORITHM

From equations (2) to (5), it can be seen that in the process of delay estimation, the following three problems are mainly faced: 1) Interference from signals sent by other base stations; 2) The influence of NLOS caused by its own multipath effect; 3) NB-IoT has a low sampling rate, which seriously affects the precision of traditional correlation delay estimation algorithms. In response to the above problems, the Inter-Cell Interference Elimination Algorithm (I_SIC) is introduced to eliminate the mutual interference between signals in multiple iterations. In each iteration, the F&T_TDE algorithm is used to estimate the delay estimation value, and the optimal delay is selected at the end of the iteration. The estimated value is substituted into the positioning solution algorithm to estimate the position coordinates of the terminal. In addition to the above three problems, in the real environment, there may be a situation where the number of positioning base stations is less than three and the algorithm may fail. Therefore, a supplementary algorithm is given in section 3.4 to deal with this special situation. When the number of base stations is greater than 3, the main body delay estimation algorithm is used, and the Chan algorithm (Chan, 1994) is used for positioning solution; otherwise, the auxiliary positioning algorithm is used. The overall idea of this article and the main body of the NB-IoT delay estimation algorithm architecture based on inter-cell interference cancellation is shown in Figure 1.

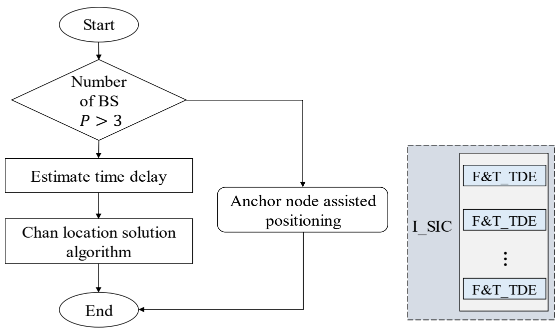

Figure 1: Proposed algorithm flowchart.

3.1 Algorithm Flow

The cell reference signal (CRS) is continuously sent, and the CRS signal sent by the serving base station is less interfered by other base station signals. Therefore, the CRS signal is used to estimate the channel of the serving base station and the user terminal before receiving the PRS signal (Weng, 2010). The method for processing the estimated time delay from each base station to the terminal is as follows: First, use the CRS signal to estimate the channel state between the serving base station and the terminal. Second, at the receiving end, receive the PRS signals from each base station, and use the existing channel state between the serving base station and the terminal to reconstruct the PRS signal of the serving cell at the receiving end, and use the F&T_TDE algorithm to estimate the time delay of the serving base station; Finally, the reconstructed PRS signal from the serving base station is subtracted from the total received PRS signal to eliminate its influence on the delay estimation of the neighboring base station. On this basis, a continuous iterative interference cancellation algorithm is used to gradually eliminate the signal between neighboring cells. At the same time, the F&T_TDE algorithm is used to estimate the delay of the serving base station.

Algorithm 1: Proposed algorithm for delay estimation.

Initialization: $\tilde{y}_{0,1}(n) \leftarrow y(n)$

```
if p = 0
  N_i ← 1, q ← 1
  Determine t̂_{0,1}
  t_0 ← t̂_{0,1}
  Determine y'_{p,q}(n)
  Obtain ỹ_{p+1,q}(n) ← ỹ_{p,q}(n) − y'_{p,q}(n)
Else
  for q = 1 to N_i
  for p = 1 to P − 1
  Determine t̂_{p,q}
  Obtain y'_{p,q}(n)
  if p < P − 1
  Obtain ỹ_{p+1,q}(n)
  Else
  ỹ_{p,q+!}(n) ← ỹ_{p,q}(n) − y'_{p,q}(n)
  end if
  p = p + 1
  end for
  q = q + 1
  end for
  t_p = min{t̂_{p,q}}
end if
```

After multiple iterations of interference elimination, the best delay estimate is selected. The pseudo-code of the main body delay estimation algorithm is shown in Algorithm 1, where $y(n)$ represents the total received signal of the device terminal; $\tilde{y}_{p,q}(n)$ and, $\hat{t}_{p,q}$ respectively represent the pth after q iterations, time-domain received signal and time delay estimation value of the cell; t_p represents the final time delay estimation value obtained by the pth cell, and N_i is the number of interference cancellation iterations.

3.2 F&T_TDE Algorithm

Inter-cell interference cancellation can only suppress the interference signals of other cells to a certain extent, and cannot solve the problem of low sampling rate of the NB-IoT system. To greatly improve the accuracy of time delay estimation, it is necessary to improve the time delay estimation algorithm. In order to improve the serial interference and avoid error propagation, before the time delay estimation is performed, the transmitted PRS signal is first based on the order of the time delay estimation from each neighboring base station to the terminal according to its energy, and then through 2 stages Gradually improve the accuracy of time delay estimation.

3.2.1 Rough Estimation of Delay Value

First, starting from the time $n_{p,l}^{0}$ (the initial time of receiving the lth OFDM symbol of the pth base station), sample the time domain signal received in the qth iteration, $\tilde{y}_{p,q}(n)$, and get N'. The received signal at the sampling point, denoted as $\tilde{y}_{p,q}^{n_{p,l}^{0}}(n)$. Secondly, using a sampling point as a sliding window, the received signal starting at $n_{p,l}^{i}$ is obtained in sequence as described above, $\tilde{y}_{p,q}^{n_{p,l}^{i}}(n)$, where, $n_{p,l}^{i} = i + lN'$, $0 \le i < N'$. Then, perform FFT transformation on $\tilde{y}_{p,q}^{n_{p,l}^{i}}(n)$ to obtain $\tilde{Y}_{p,q}^{n_{p,l}^{0}}(k), \tilde{Y}_{p,q}^{n_{p,l}^{1}}(k), \ldots, \tilde{Y}_{p,q}^{n_{p,l}^{N'}}(k)$ and perform the local positioning reference signal corresponding to the l OFDM symbol of the p base station with $\tilde{Y}_{p,q}^{n_{p,l}^{i}}(k)$ frequency-domain correlation operation is performed to obtain the corresponding OFDM symbol l_p' and delay number $n_{p,l}'$ when the correlation function of the base station p is maximized, as shown in equation (7).

$$[n_{p,l}', l_p'] = \underset{n_{p,l}', l}{\arg\max} \left\{ \sum_{k=0}^{N'-1} \left| S_{p,l}(k) \left(\tilde{Y}_{p,q}^{n_{p,l}^{i}}(k)(k - n_{p,l}^{i}) \right)^{*} \right| \right\} \quad (7)$$

Among them, when $p = 0$, $q = 1$, and $p > 0$, and $q \in \{1,2,\ldots,N_i\}$; N_i represents the total number of iterations of the continuous interference cancellation algorithm. $n_{p,l}' - n_{p,l}^{0}$, which is the number of delays in the rough estimate of the qth iteration. Since noise and multipath effects will cause NLOS effects, the time delay value obtained at this time has a large error, so this paper uses the first path search algorithm to reduce the error. The specific implementation process of the algorithm is as follows.

Before the signal arrives, the receiver first collects the noise signal and converts it into a frequency domain signal $W_{\varphi}(k)$, and correlates it with the local PRS signal in the frequency domain, repeats Φ times, and obtains the average value as shown in equation (8) (mean noise floor).

$$\bar{R}_{\mathrm{SW}} = \frac{1}{\Phi} \sum_{\varphi}^{\Phi} \sum_{k=0}^{N'-1} \left| S_{p,l_p'}(k) W_{\varphi}^{*}(k) \right| \quad (8)$$

Set the noise floor threshold as L_{limit}^{p}, the noise floor threshold and the average value of the noise floor should satisfy the relationship shown in equation (9), where the industrial setting $\kappa = 6$ dB and is expressed as

$$\kappa = 10 \log \frac{L_{\mathrm{limit}}^{p}}{\bar{R}_{\mathrm{SW}}} \quad (9)$$

The frequency domain received signal corresponding to the OFDM symbol l_p' with the largest peak value obtained by the rough estimation of the time delay value, $\tilde{Y}_{\mathrm{p,q}}(k)$ is correlated with the local PRS signal in the frequency domain to obtain the correlation function, $R_{S_p,\tilde{Y}_{p,q}}(k)$, where $k \in [l_p' N', (l_p'+1)N']$.

$$R_{S_p,\tilde{Y}_{p,q}}(k) = R_{\mathrm{signal}}^{p}(k) + R_{\mathrm{noise}}^{p}(k) \quad (10)$$

Among them, $R_{\mathrm{signal}}^{p}(k)$ represents the correlation function between the useful signal and the interference signal and the local PRS signal, and $R_{\mathrm{noise}}^{p}(k)$ represents the correlation function between the noise and the local PRS signal. In order to accurately estimate the required cell delay value, it is necessary to eliminate the influence of the interference signal, so the noise floor threshold is introduced to obtain the $\hat{R}_{\mathrm{noise}}^{p}(k)$ shown in equation (11).

$$\hat{R}^{p}_{\text{noise}}(k) = \frac{R_{S_p,Y_{p,q}}(k)}{\max\left\{R_{S_p,Y_{p,q}}(k)\right\}} L^{p}_{\text{limit}} \tag{11}$$

When the amplitude of the first path signal is small, the useful signal will be overwhelmed by noise and interference signals, and it is impossible to determine the final required delay estimate based on the first path delay value. Therefore, an amplitude threshold α is set. When the amplitude of the first arrival path is less than the threshold, a suboptimal path will be selected, and the instant delay value is only greater than the path of the first arrival path, thus the first arrival path search formula can be obtained as (12) shown.

$$\tilde{n}_{p,q} = \underset{k}{\arg\min}\left\{R_{S_p,\tilde{y}_{p,q}}(k) > \alpha\left\{\max\left\{R_{S_p,\tilde{y}_{p,q}}(k)\right\} \frac{R_{S_p,\tilde{y}_{p,q}}(k)}{\max\left\{R_{S_p,\tilde{y}_{p,q}}(k)\right\}} L^{p}_{\text{limit}}\right\}\right\} \tag{12}$$

Among them, $\tilde{n}_{p,q}$ is the delay number of the first path.

3.2.2 Time Delay Fine Estimation Stage

First, let, $v_{p,q} \in \left[\tilde{n}_{p,q} - \Delta\mu, \tilde{n}_{p,q} + \Delta\mu\right]$, the value of $v_{p,q}$ is $\frac{2\Delta\mu}{\omega}$; Secondly, for the time-domain received signal corresponding to the l'_p OFDM symbol, $\tilde{y}_{p,q}\left(v_{p,q} + \frac{2i\Delta\mu}{\omega}\right)$ interpolates to obtain the signal $\bar{y}^{v_{p,q}}_{p,q}$, where $i \in \{0,1,\ldots,N'-1\}$, interpolation function set. The expression is shown in equation (13).

$$\bar{y}^{v_{p,q}}_{p,q}(i) = \begin{cases} \tilde{y}_{p,q}(\text{floor}(\psi)) & \text{floor}(\psi) < \psi < \text{ceil}(\psi) - 0.5 \\ \tilde{y}_{p,q}(\text{ceil}(\psi)) & \text{ceil}(\psi) - 0.5 < \psi < \text{ceil}(\psi) + 0.5 \end{cases} \tag{13}$$

Among them, $\psi = v_{p,q} + \frac{2i\Delta\mu}{\omega}$, $\text{floor}(\psi)$ represents rounding ψ to the $-\infty$ direction, $\text{ceil}(\psi)$ represents rounding ψ to the $+\infty$ direction, $\Delta\mu$ represents the selected time-domain interpolation range, and ω represents the number of points for time domain interpolation.

The processed received signal $\bar{y}^{v_{p,q}}_{p,q}(i)$ is correlated with the local PRS signal corresponding to the selected base station p in the time domain, and the accurate time delay estimation value from the pth base station to the terminal at the qth iteration is obtained, $\hat{t}_{p,q}$, as in equations (14) as shown.

$$\begin{cases} \hat{\imath}_{p,q} = \underset{i}{\arg\text{maz}} E\left[S_{p,l'_p}(i + l'_p N')\bar{y}^{v_{p,q}}_{p,q}(i)\right] \\ \hat{t}_{p,q} = \tilde{n}_{p,q} - \Delta\mu + \frac{2\Delta\mu\hat{\imath}_{p,q}}{\omega} - l'_p N' \end{cases} \tag{14}$$

We use the channel estimation algorithm described in below section to obtain the channel state between the base station p and the terminal, and reconstruct the received signal from the base station,$y'_{p,q}(n)$, and subtract from the received signal, $\tilde{y}_{p,q}(n)$ is the reconstructed signal obtains equations (15) and (16).

If $p < P - 1$, then

$$\tilde{y}_{p+1,q}(n) = \tilde{y}_{p,q}(n) - y'_{p,q}(n) \tag{15}$$

If $p = P - 1$ and $q \leq N_i$, then

$$\tilde{y}_{p,q+1}(n) = \tilde{y}_{p,q}(n) - y'_{p,q}(n) \tag{16}$$

3.2.3 Channel Estimation

In order to reduce the computational complexity of the algorithm, this paper uses the least square method to estimate the channel of the positioning reference signal from the base station p to the user terminal. When $p = 0$, channel estimation is performed on the CRS signal of the serving base station, and the system function is obtained as shown in equation (17).

$$\boldsymbol{H}_{\text{CRS},l} = \boldsymbol{S}^{-1}_{\text{CRS},l}\boldsymbol{Y}_{\text{CRS}} \tag{17}$$

Among them, $\boldsymbol{Y}_{\text{CRS}}$ and $\boldsymbol{S}_{\text{CRS},l}$ respectively represent the CRS signal received by the terminal and the CRS signal sent by the serving base station. Perform linear interpolation on this system function (Bohanuding (2010)) to obtain the channel estimation of the time-frequency position of the PRS signal, and perform IFFT transformation on it to obtain $h_{0,1}(i + lN')$, where $i = 0,1,2,\ldots,N'-1$. The reconstructed signal from the serving base station is

$$y'_{0,1}(n) = \sum_{l=0}^{L-1} h_{0,1}(n)\, S_{p,l}\left(n - \left[\tilde{v}_{0,1}\right]\right) \tag{18}$$

Where, $n \in [lN', (l+1)N']$.

At this time, $p > 0$, and the system function is obtained as shown in equation (19).

$$h_{p,q}(i + lN') = \text{IFF}\frac{Y_{p,q}(k)}{S_{p,l}(k)} \tag{19}$$

According to the system function shown in equation (19), the received signal from the base station p is reconstructed, and the reconstructed signal is

$$y'_{p,q}(n) = \sum_{l=0}^{L-1} h_{p,q}(n)\, S_{p,l}\left(n - \left[\hat{v}_{p,q}\right]\right) \tag{20}$$

Where, $n \in [lN', (l+1)N']$.

3.2.4 Anchor Node Location Algorithm

The DV-Hop positioning algorithm is one of the key technologies for anchor node positioning. It adopts a distance vector-hop mechanism, does not need to measure the distance between nodes, and does not require additional hardware support. It is a distance-independent (range- free) algorithm. This article chooses DV-Hop algorithm as the auxiliary positioning algorithm. For areas with less deployment of base stations, when the number of base stations is less than 4 (the position estimation deviation is relatively large when the number of base stations is 3), the terminal device node broadcasts a positioning data packet to the anchor node, and the anchor node records the receiving time of receiving the data packet Stamp and the ID of the terminal node to be located. At the same time, the anchor nodes perform time synchronization through satellite navigation and obtain terminal device node geographic location data and store it in the background server to provide relevant parameters for algorithm processing. Each anchor node sends a new data packet to the gateway, and the gateway forwards the new data packet to the background server, and uses the weighted centroid algorithm to estimate the position coordinates of the terminal node (Qiang (2020)). It should be noted that the anchor node location algorithm, as an auxiliary part of the algorithm proposed in this article, only works when the main algorithm fails.

4 SIMULATION RESULTS

This section provides the numerical simulation results with elaboration. The proposed algorithm is evaluated from different important aspects.

4.1 Simulation Parameters Settings

During the simulation, due to the synchronous network mode, the wireless subframes sent by all base stations are aligned in the time domain. Since the NB-IoT network is mainly for macroscopic and low-speed objects, the simulation assumes that the device terminal. The moving speed is 0 km/s, and other simulation parameters are set according to the PRS signal in 3GPP R14 and based on the OTDOA positioning method (Mwakwata (2019)). The specific parameter settings are shown in Table 1. The NB-IoT device terminal nodes (solid nodes) scattered in the dark gray area are randomly selected, and m anchors are fixed in a grid in each 500 m × 500 m area node and configure the GNSS positioning module as a reference node for positioning. When the number of base stations involved in positioning is less than 4, anchor node positioning is enabled. When studying the influence of distance on time delay estimation, the equipment terminal in the direction 1 area as shown in Figure 2(b) is selected. In addition, select the 4 base stations closest to the terminal as the positioning base station, where base station 0 (located in the center of the serving cell) is the serving base station, and base station 1/2/3 (located in the center of the neighboring cell 1/2/3) is the neighboring base station.

Table 1: Simulation Parameters.

Parameter	Value
Number of BS and NB-IoT antennas	1
Number of terminal nodes	5000
Number of base stations	4
Base station spacing	1732 m
Moving speed of terminal equipment	0 km/s
N_{PRS}	1
N_i	3
CP type	Conventional CP
Sampling rate F_s	1.92 MHz
Δt	$1/F_s$
$2\Delta\mu/\omega$	0.01
Path loss	$L_d = 120.9 + 37.6\ d$
Channel model	AWGN

In the simulation, the delay estimation based on the positioning reference signal mainly uses the detection probability (PD) of the delay estimate, the root mean square error (RMSE) of the delay estimation and the cumulative distribution function (CDF) of the device terminal positioning error. To measure the positioning effect, the positioning error is mainly used to measure the auxiliary positioning based on anchor nodes.

4.2 Simulation Results Analysis

4.2.1 Probability of Detection

In this paper, the detection probability refers to the probability that the estimated time delay $\hat{t}$ is within a given threshold T in M Monte Carlo simulation experiments. In order to satisfy that users participating in positioning are located within the coverage of the serving base station, the threshold here is $T_{\text{threshold}} = 5.78 \times 10^{-6}$s, the instant delay error is less than the propagation time of the signal from two adjacent base stations. In Figure 2, the number of Monte Carlo simulations is set to 1,000, and the detection probability PD of the serving cell and neighboring cell 1 are given as a function of SNR. As shown in Figure 2(a), when the SNR is greater than 20 dB, the detection probability shows an obvious upward trend; when the SNR is less than −12 dB, due to the influence of noise, the detection probability of the serving cell obtained by the proposed algorithm and the two comparison algorithms Very low, and when the signal-to-noise ratio of the proposed algorithm is too low, the

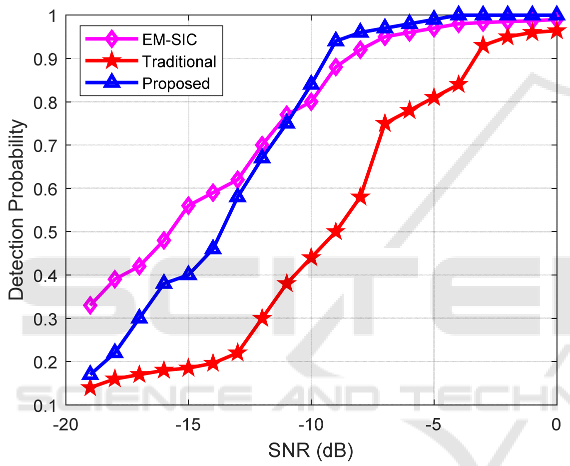

(a) Comparison of detection probability of serving cell

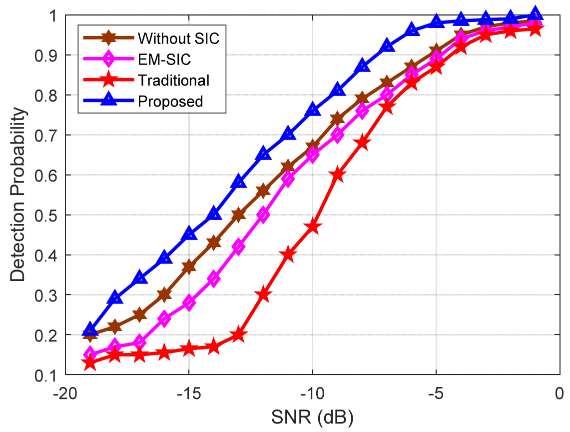

(b) Comparison of detection probability of neighboring cell 1

Figure 2: Serving cell and neighboring cell 1 detection probability varies with SNR.

reconstruction signal error is too large, which seriously affects the delay estimation, and the detection probability is lower than the EM-SIC algorithm; when the SNR is greater than −12 dB, the detection probability will exceed EM-SIC algorithm; In addition, compared with the other two algorithms, the proposed algorithm has a more significant upward trend in the detection probability curve. Similarly, as shown in Figure 2(b), for neighboring cell 1 (the curve trend of neighboring cells 2/3 and 1 is basically the same), when the SNR is greater than −20 dB, as the SNR increases, the detection probability becomes obvious Increasing trend, and the detection probability of the proposed algorithm is higher than that of the EM-SIC algorithm and the traditional algorithm; in order to highlight the effect of inter-cell interference elimination, Figure 2(b) also shows that the interference is not added.

In the case of elimination, it can be seen that adding interference elimination can effectively improve the detection probability.

4.2.2 RMSE Analysis

The definition of the root mean square error is shown in equation (21).

$$RMSE = c\sqrt{\frac{1}{M}\sum_{1}^{M}(\hat{t}-t)^2} \tag{21}$$

Among them, c is the speed of light, and the value is 3.0×10^{8} m/s; M is the number of Monte Carlo simulations and the value is 1 000; t is the actual delay value. In addition, the CRLB lower bound (CRLB) provides a measure of the error of the delay estimation. From the literature (Xu (2016)), the CRLB lower bound of the NB-IoT delay estimation in the AWGN environment can be expressed as

$$var\{\hat{t}\} \geq \text{CRLB}\{\hat{t}\} = \frac{\sigma^2}{8\pi^2 \Delta f \sum_{l=}^{L}\sum_{k=0}^{N-1} k^2 \left|s_{p,l}(k)\right|^2} \tag{22}$$

where, $\Delta f = 1/NT_s$ and σ^2 is the noise power.

The mean square error of the delay estimation can be used to measure the accuracy of the delay estimation.

Figure 3(a) compares the mean square error of the delay estimation of the serving cell. Since the proposed algorithm uses the channel estimation of the cell reference signal to reconstruct the positioning reference signal of the serving cell, the obtained delay estimated value is obviously closer to the CRLB lower bound than the traditional correlation algorithm and the EM-SIC algorithm.

In addition to SNR affecting the delay estimation result, the distance between the positioning terminal and the serving base station and neighboring base stations also affects the delay estimation.

In Figure 3(b), the influence curve of the distance between the serving base station and the positioning terminal (along direction 1 in Figure 2(b)) on the delay estimation is given when SNR=5 dB. It can be seen that when the distance is small, the mean square error of the serving cell is relatively small, while neighboring cells are seriously affected by the serving cell, and the mean square error of the time delay estimation is relatively large. As the distance increases, the mean square error of the serving cell gradually increases, while the mean square error of neighboring cells gradually decreases. Therefore, the importance of inter-cell interference cancellation is explained from the perspective of the influence of distance on time delay estimation.

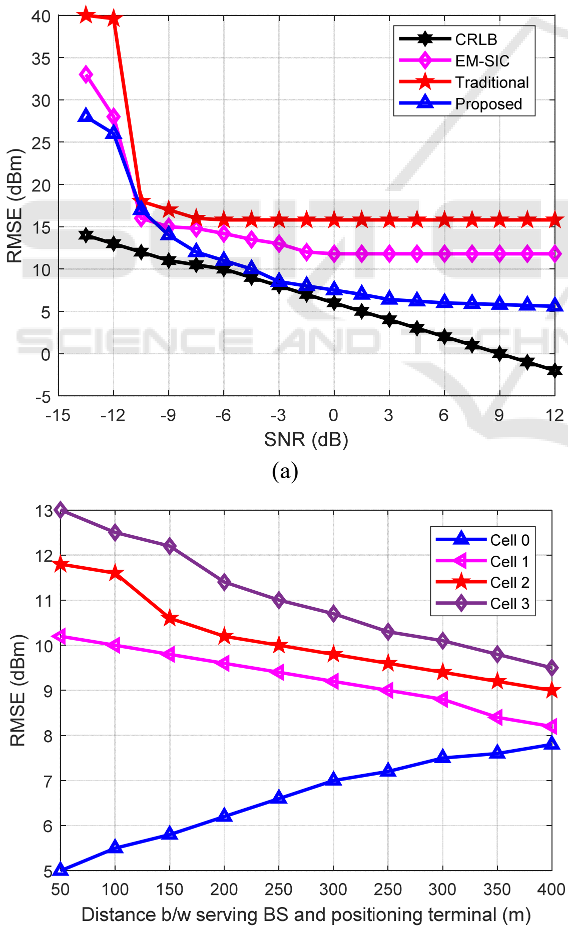

(a)

(b)

Figure 3: Time delay estimation mean square error variation curve of cell 0/1.

4.2.3 CDF of Positioning Error

When the positioning solution method is determined, the positioning accuracy of the user terminal is determined by the accuracy of the delay estimation, that is, it is jointly determined by multiple delay estimation values (the delay estimation values from 3 or more base stations to the user terminal). The simulation in this paper uses the Chan algorithm to solve the problem, which can reach the CRLB lower bound when the delay estimation error is small.

Figure 4 shows the comparison of the positioning error curves of the traditional algorithm, the algorithm proposed in this paper, and the EM-SIC algorithm. It can be seen from Figure 4 that the positioning accuracy of the algorithm in this paper is significantly higher than the traditional algorithm and the EM-SIC algorithm. This is because the algorithm proposed in this paper incorporates interference cancellation, which improves the positioning accuracy of the algorithm to a certain extent.

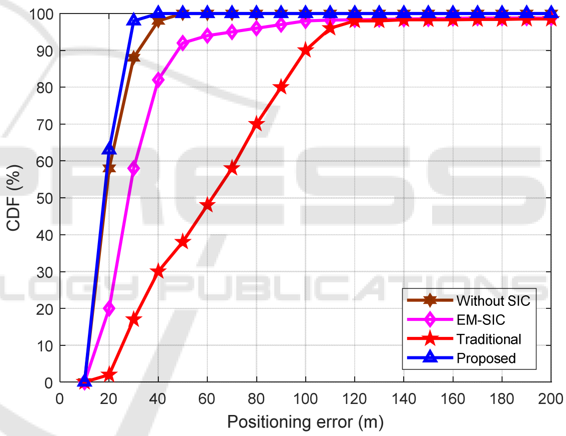

Figure 4: Comparison of positioning error and CDF.

Table 2 shows the positioning errors of different algorithms for different cumulative errors. As shown in Table 2, when the cumulative error reaches 50%, the positioning error of this algorithm can reach 4.27 m, while the traditional algorithm positioning error is 47.56 m, and the EM-SIC algorithm positioning error is 18.52 m; when the cumulative error reaches 90%, the gap between the three is even greater.

Table 2: Analysis of positioning error corresponding to different accumulated errors.

Algorithm	**CDF**		
	50%	80%	90%
Traditional algorithm	47.56 m	69.46 m	81.18 m
EM-SIC algorithm	18.52 m	28.73 m	39.50 m
Proposed algorithm without IC	5.52 m	8.73 m	10.88 m
Proposed algorithm with IC	4.27 m	6.56 m	8.00 m

4.2.4 Aided Positioning Simulation Analysis

Figure 4 shows the analysis of anchor node positioning error. It can be seen that the number of anchor nodes and the communication radius of the nodes will affect the accuracy of positioning. When the communication radius of the node is 60 m, the relationship between the number of anchor nodes and the positioning error is shown in Figure 3(a). As the number of anchor nodes increases, the positioning error gradually decreases, but at the same time, positioning cost also increases. The communication radius and the density of anchor nodes also restrict each other. When the location of the anchor node is determined, the distance between the nodes is also determined. The communication radius will affect the average hop distance of the algorithm, thereby affecting the positioning accuracy. At this time, the positioning error of the communication radius first decreases and then gradually increases. The position of the turning point is determined by the communication radius and the density of anchor nodes. Figure 3(b) shows the relationship between communication radius and positioning error when there are 64 anchor nodes. It is worth noting that the increase in the communication radius is obtained by increasing the transmission power.

From the above simulation analysis, it can be seen that to improve the positioning accuracy of the auxiliary positioning algorithm, the number of anchor nodes and the communication radius need to be increased. At this time, the positioning cost will also increase year-on-year. However, the position estimation effect of the auxiliary positioning algorithm is far less than that mentioned in this article. Delay estimation algorithm, so the auxiliary positioning algorithm is only used as a backup solution when the base station is insufficient in real positioning scenarios.

5 CONCLUSION

This article proposes a delay estimation algorithm based on inter-cell interference cancellation for the problems of NB-IoT's cost limitation and low sampling rate. The algorithm continues the low complexity advantages of the traditional cross-correlation algorithm, and uses base stations to participate in positioning to reduce equipment overhead, and more satisfies the low power consumption and low cost characteristics of NB-IoT. Through simulation analysis, the proposed delay estimation algorithm can effectively suppress the influence of inter-cell interference and NLOS. The delay estimation accuracy is significantly higher than the comparison algorithm, which is more in line with today's high-precision location sensing needs. As to whether there are positioning scenarios with SNR less than −20dB and whether it is necessary to improve the TDE accuracy below −20dB, further research is needed.

ACKNOWLEDGMENT

The authors would like to thank the editors and reviewers for their review and recommendations.

REFERENCES

K. Staniec, M. Kucharazak, Z. Joskiewics and B. Chowanski, “Measurement-Based Investigations of the NB-IoT Uplink Performance at Boundary Propagation Conditions,” *Electronics*, vol. 9, no. 11, pp. 1–13, 2020.

C. Knapp and G. Carter, “The Generalized Correlation Method for Estimation of Time Delay,” *IEEE Transactions on Acoustic Speech & Signal Processing*, vol. 24, no. 4, pp. 320–327, 2003.

Z. Deng, X. Zheng, H. Wang, X. Fu, L. Yin *et al*., “A Novel Time Delay Estimation Algorithm for 5G Vehicle Positioning in Urban Canyon Environments,” *Sensors*, vol. 20, no. 18, pp. 1–19, 2020.

O. A. Saraereh, A. Alsaraira, I. Khan and B. J. Choi, “A Hybrid Energy Harvesting Design for On-Body Internet-of-Things (IoT) Networks,” *Sensors*, vol. 20, no. 2, pp. 1–13, 2020.

Y. Gu and N. A. Goodman, “Information-theoretic compressive sensing kernel optimization and Bayesian Cramer-rao bound for time delay estimation,” *IEEE Transactions on Signal Processing*, vol. 65, no. 17, pp. 4525–4537, 2017.

W. Shahjehan, S. Bashir, S. L. Mohammed, A. B. Fakhri, A. D. Isaiah *et al*., “Efficient Modulation Scheme for Intermediate Relay-Aided IoT Networks,” *Applied Sciences*, vol. 10, no. 6, pp. 1–14, 2020.

B. M. Lee, M. Patil, P. Hunt and I. Khan, “An Easy Network Onboarding Scheme for Internet of Things Networks,” *IEEE Access*, vol. 7, pp. 8763–8772, 2018.

I. Khan and D. Singh, “Energy-balance node-selection algorithm for heterogeneous wireless sensor networks,” *ETRI Journal*, vol. 40, no. 5, pp. 604–612, 2018.

S. Hu, A. Berg, X. Li and F. Rusek, “Improving the Performance of TDOA Based Positioning in NB-IoT Systems,” *IEEE Global Communications Conference* (GLOBECOM), Singapore, pp. 1–7, 2017.

D. Ye, J. Y. Lu, X. J. Zhu and H. Lin, “Generalized Cross Correlation Time Delay Estimation Based on Improved Wavelet Threshold Functionn,” *IEEE 6th International Conference on Intrumentation & Measurement,* *Computer, Communication and Control (IMCCC)*, Harbin, China, pp. 629–633, 2016.

H. M. Sun, R. S. Jia, Q. Q. Du *et al*., "Cross-correlation Analysis and Time Delay Estimation of a Homologous Micro-Seismic Signal Based on the Hilbert-Huang Transform," *Computers & Geosciences*, vol. 91, no. C, pp. 98–104, 2016.

F. Jameel, T. Ristaniemi, I. Khan and B. M. Lee, "Simultaneous Harvest-and-Transmit Ambient Backscatter Communications Under Rayleigh Fading," *EURASIP Journal on Wireless Communications and Networking*, vol. 166, pp. 1–9, 2019.

T. Jabeen, Z. Ali, W. U. Khan, F. Jameel, I. Khan *et al*., "Joint Power Allocation and Link Selection for Multi-Carrier Buffer Aided Relay Network," *Electronics*, vol. 8, no. 6, pp. 1–13, 2019.

Y. T. Chan and K. C. Ho, "A Simple and Efficient Estimator for Hyperbolic Location," *IEEE Transactions on Signal Processing,* vol. 42, no. 8, pp. 1905–1915, 1994.

G. Weng, C. Yin and T. Luo, "Channel Estimation for the Downlink of 3GPP-LTE systems," *IEEE International Conference on Network Infrastructure and Digital Contents*, Beijing, China, pp. 1042–1046, 2010.

S. Bohanuding, M. Ismail and H. Hussai, "Simulation Model and Location Accuracy for Observed Time Difference of Arrival (OTDOA) Positioning Technique in Third Generation System," *IEEE Student Conference on Research and Development – Engineering: Innovation and Beyond*, Putrajaya, Malaysia, pp. 63–65, 2010.

L. Qiang, H. Xia, X. Yuhang and Z. Dan, "Improved DV-Hop Based on Dynamic Parameters Differential Evolution Localization Algorithm," *IEEE 8th International Conference on Information, Communication and Networks (ICICN)*, Xi'an, China, pp. 129–134, 2020.

C. B. Mwakwata, H. Malik, M. M. Alam, Y. L. Moullec, S. Parand *et al*., "Narrowband Internet of Things (NB-IoT): From Physical (PHY) and Media Access Control (MAC) Layers Perspective," *Sensors*, vol. 19, no. 11, pp. 1–34, 2019.

W. Xu, M. Huang, C. Zhu, *et al*., "Maximum Likelihood TOA and OTDOA estimation with first arriving path detection for 3GPP LTE system," *Transactions on Telecommunications Technologies*, vol. 27, no. 3, pp. 339–356, 2016.